Compact Wideband Dual-Band SIW Bandpass Filters

Yun Jiang, Lei Huang*, Zhaoyu Huang, Yuan Ye, Boyuan Liu, Wentao Yuan, and Naichang Yuan

State Key Laboratory of Complex Electromagnetic Environment Effects on Electronics and Information System
College of Electronic Science, National University of Defense Technology, Changsha, 410073, China
*huanglei_nudt@163.com

Abstract ─ A novel method to design compact wideband dual-band substrate integrated waveguide (SIW) bandpass filters (BPF) is proposed in this paper. By loading a novel beeline compact microstrip resonant cells (BCMRCs) with band-gap characteristics on top layer of SIW, two wide passbands separated by a stopband are generated. In order to enable the filter to have lower reflection coefficients in the two passbands, we use a tapered gradient line embedded with rectangular slots and loaded open stubs as the transition structure from microstrip line to SIW. The wideband dual-band BPF (DBBPF) is fabricated. The lower-band and upper-band fractional 3-dB bandwidths are 58.2% and 22.6%, while the measured minimum insertion losses (ILs) are 0.7 and 0.92 dB, respectively. The stepped-impedance open-loop ring resonator (SIOLRR) is introduced in order to improve the selectivity of the filter. The wideband DBBPF with SIOLRR is studied, simulated and measured. Two transmission zeros are generated in the stop band between the two passbands. Good agreement between simulated and measured results can be obtained.

Index Terms ─ Complementary split ring resonators, defected ground structure, dual-band bandpass filter, stepped-impedance open-loop ring resonator, substrate integrated waveguide.

I. INTRODUCTION

With the rapid development of wireless communication technologies, frequency spectrum resources have become increasingly scarce, thus dual-band system have received more and more attention. As an important passive component of wireless communication, DBBPF has been widely studied and developed [1-6]. But up to now, most DBBPFs are based on microstrip technology. Although they are simple structure and low in cost, disadvantages such as low power-banding capacity and poor performance limit their application [7-9]. Waveguide filters and dielectric resonator filters can effectively overcome the shortcomings mentioned above, but they are costly and bulky [10]. Fortunately, a new planar integration scheme called substrate integrated waveguide (SIW) has emerged and attracted tremendous attentions. It is a type of waveguide-like structure which enjoys not only the advantages of classical rectangular waveguide features, but also the benefits of planar circuit, thereby providing a promising platform to develop excellent filters which can satisfy the stringent requirements of modern wireless communication systems [11-13]. In [14] a dual-band SIW filter is obtained by loading E-shaped defected ground structure (DGS) on either top or bottom sides. In [15], two same or different sized complementary split ring resonators (CSRRs) are etched on the top side of SIW cavity to achieve a dual-band frequency response. The dual-band balanced SIW bandpass filter is demonstrated in [16], by vertically cascading two square SIW cavities. However, the all dual-band SIW filters mentioned above are narrow-bandwidth. As a result, they are not suitable in broadband wireless communication systems.

This paper presents a novel method to design compact wideband SIW DBBPFs. It combines the SIW and BCMRC technologies, which allow the implementation of two wide passbands. In order to improve the selectivity of the wideband SIW DBBPFs, the SIOLRRs are loaded on the input and output ports of the filter. Detailed working mechanisms and design method are explained as follows. For verification, two wideband SIW DBBPFs are proposed, fabricated and measured.

II. DUAL-BAND BANDPASS FILTERS STRUCTURE AND DESIGN

Figure 1 depcits the configuration and optimal physical parameters of the wideband DBBPF with SIOLRR. It directly excited by two 50 Ω standard microstrip feeding lines. The SIW structure consists of a dielectric substrate comprised between a pair of metal plates which are connected through via holes. The used substrate is Rogers 4350B with the thickness h=0.508 mm and its bottom is covered completely by a metal. A periodic BCMRCs unit is loaded on the top layer of the SIW. Electromagnetic waves are confined to the inside of

Submitted On: March 7, 2021
Accepted On: May 9, 2021
https://doi.org/10.47037/2021.ACES.J.360919

SIW cavity, hence it can be considered as a planar circuit transformation of non-planar rectangular waveguide (RGW). If the electromagnetic waves are lower than the cutoff frequency, it will not be able to propagate in the SIW cavity. Since a periodic BCMRCs structure usually presents stopband characteristics, a compact DBBPF is obtained by combining the characteristics of SIW and BCMRCs. The DBBPF can be considered as a cascade connection of a highpass filter with a bandstop filter to form dual-passbands separated by a stopband, and the bandwidth of dual passbands is mainly determined by BCMRCs.

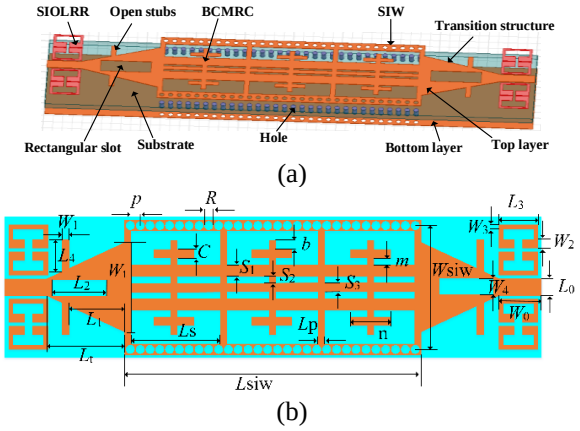

Fig. 1. Configuration of the wideband DBBPF with SIOLRR: (a) three-dimensional (3D) view, (b) planar view, where b=0.7 mm, C=0.5 mm, R=0.5 mm, p=0.9 mm, m=0.3 mm, n=1.5 mm, S_1=1.2 mm, S_2=0.3 mm, S_3=0.5 mm, W_0=3.5 mm, W_1=0.5 mm, W_2=0.75 mm, W_3=0.2 mm, W_4=1.7 mm, W_t=6.3 mm, W_{siw}=8.7 mm, Ls=8.37 mm, L_{siw}=27.1 mm, L_p=0.495 mm, L_t=2.6 mm, L_1=4.5 mm, L_2=5.2 mm, L_3=3 mm, L_4=1.675 mm.

A novel beeline structure is shown in Fig. 2, which is composed of five horizontal microstrip lines and one vertical microstrip line, and the three horizontal microstrip lines in the middle are connected in parallel and run through the entire unit structure. With the help of 3D simulation software HFSS, the simulated frequency response of a novel periodic BCMRCs unit with three beeline structure is shown in Fig. 3. As seen in Fig. 3, the BCMRCs structure plays not only the role of a low-pass, but also produces a passband.

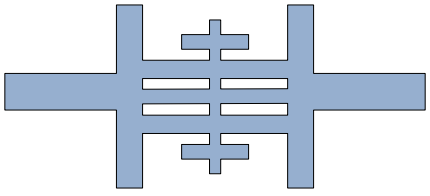

Fig. 2. The novel beeline structure.

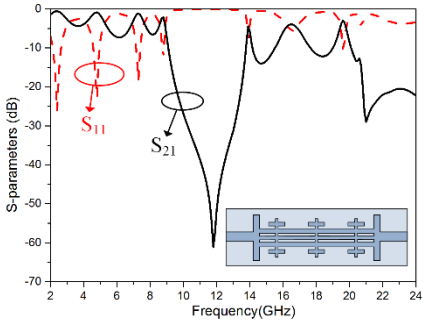

Fig. 3. Simulated results of a novel periodic BCMRCs unit.

It is well known that a SIW is similar to a RGW as a high-pass filter. According to the theory of typical RGW, the cutoff frequency of the fundamental mode in the SIW cavity can be calculated as:

$$f_{c10} = \frac{c}{2\sqrt{\varepsilon_r \mu_r}} \sqrt{\frac{1}{\left(W_{SIW} - \frac{d^2}{0.95p}\right)^2}}, \tag{1}$$

where c is the light velocity in vacuum, ε_r and μ_r are relative permittivity and relative permeability, W_{SIW} is the spacing between the rows of two metallic vias on the SIW, d is the diameter of metalized vias and p is the center-to-center pitch between adjacent via-holes. In addition, since the SIW is not an ideal homogenous rectangular waveguide, the gap between the aligned metallic vias may trigger frequency-dependent leakage loss. To prevent radiation loss, the parameters of the typical SIW structure must be sustained to meet the following condition [17]:

$$\begin{cases} d < 0.2\lambda_g \\ d < 0.2W_{SIW} \\ d > 0.5p \end{cases}. \tag{2}$$

Where λ_g can be calculated by:

$$\lambda_g = \frac{\lambda_0}{\sqrt{1 - \left(\frac{\lambda_0}{2\left(W_{SIW} - d^2/0.95p\right)}\right)^2}}, \tag{3}$$

where λ_0 is the free space wavelength. According to the target specifications and these relations mentioned above, all the examples presented in this paper are designed with d=0.5 mm and p=0.9 mm.

In order to verify the proposed design method, the prototype DBBPF is simulated by full-wave simulator HFSS. As seen in Fig. 4, due to the slow wave effect produced by the loaded BCMRCs, the cutoff frequency of the SIW of the same size has been moved from 9.7 GHz to 4.4 GHz. According to (1), the loaded BCMRCs reduces the equivalent width of SIW by about 55%. At

the same time, by loading the BCMRCs with band-gap characteristics on top layer of SIW, two wide passbands separated by a stopband are generated.

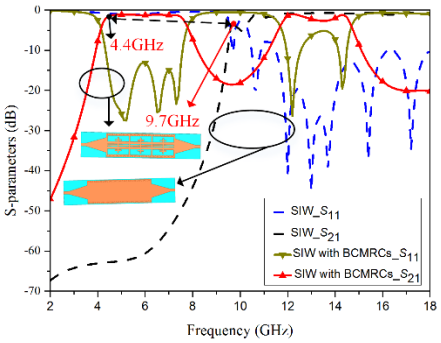

Fig. 4. Simulated S-parameters of the initial SIW and the SIW with BCMRCs.

In order to enable the wide DBBPF to have lower reflection coefficients, a tapered gradient line embedded with rectangular slots and open stubs are introduced. The simulated results of the dual-band filter with or without rectangular slots and open stubs in Fig. 5. As seen in Fig. 5, by loading rectangular slots and loaded open stubs on the transition structure of microstrip-SIW, the return losses of the two passbands are better than 10 dB.

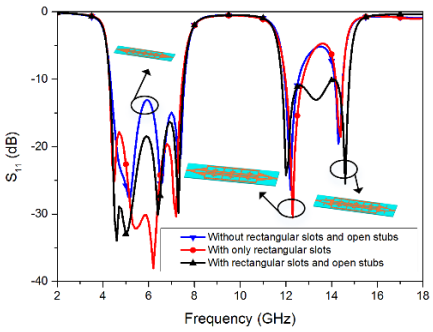

Fig. 5. Simulated frequency responses of the DBBPF with or without rectangular slots and open stubs.

The simulated results of the wideband DBBPF with rectangular slots and open stubs is shown in Fig. 6. The lower passband is from 4.2 GHz to 7.65 GHz, while the upper passband frequency covers from 11.65 GHz to 14.85 GHz. The simulated 3dB fractional bandwidths are 58.2% and 24.2%, and the return losses of the two passbands are below 10dB, respectively. The center frequency and bandwidth of the two passbands can be flexibly adjusted in this filter. As seen in Fig. 7, the bandwidth of two passbands decreases as m increases, while the upper passband has a greater change than the lower passband. Moreover, if L_s increases, the bandwidth of the two passbands becomes lager, but the lower passband changes more than the upper passband.

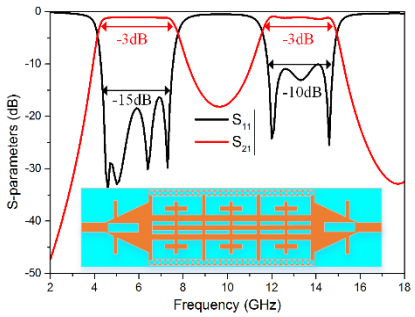

Fig. 6. Simulated results of the wideband DBBPF.

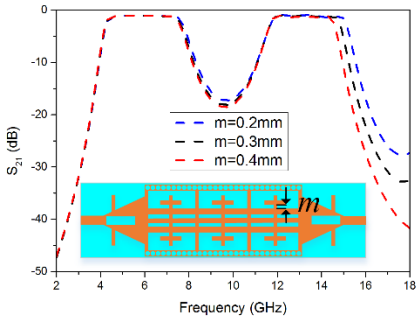

(a)

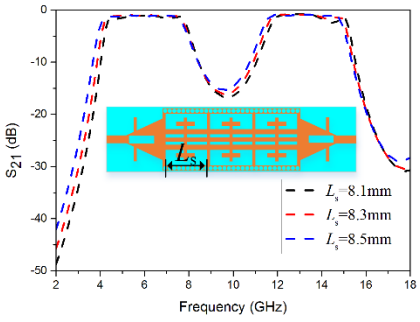

(b)

Fig. 7. Simulated frequency responses of: (a) m and (b) L_s.

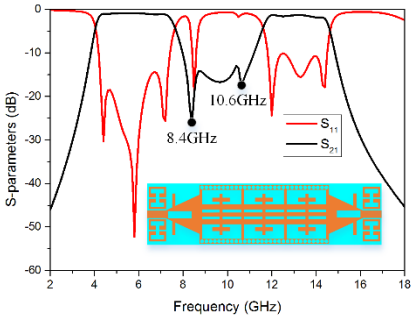

Fig. 8. Simulated frequency responses of the wideband DBBPF with SIOLRR.

However, the DBBPF have poor frequency selectivity between two bands. In order to improve the frequency selectivity, the SIOLRRs is loaded on both sides of the input and output ports of the filter, and its frequency response results are shown in Fig. 8. As seen in Fig. 8, two transmission points are generated in the stop band between the two passbands, and it is obvious that the wideband DBBPF with SIOLRR has a better frequency selectivity.

III. EXPERIMENTAL RESULTS

According to the analysis and discussion above, the two prototype wideband DBBPFs are designed, fabricated and measured. Figure 9 shows the photograph of the fabricated filters. The overall circuit size of the DBBPF is 9.7 mm×45.7 mm (0.26 λ_g×1.22 λ_g), and the size of the DBBPF with SIOLRR is 9.7 mm×49.7 mm (0.26 λ_g×1.35 λ_g), where λ_g is the guided wavelength in the substrate at center frequency (CF) of the first passband.

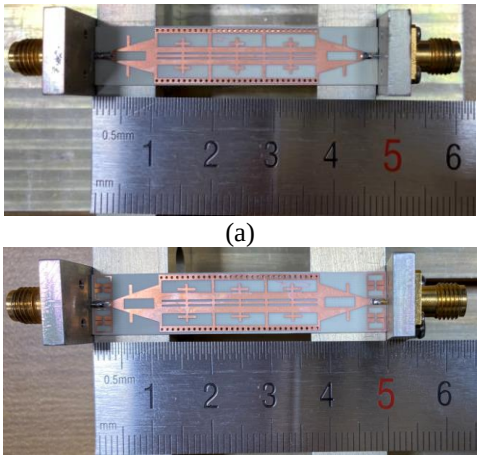

(a)

(b)

Fig. 9. Photograph of the fabricated DBBPFs: (a) the DBBPF without SIOLRR, and (b) the DBBPF with SIOLRR.

The simulated and measured results are shown in Fig. 10. In Fig. 10 (a), the lower-band and upper-band of the proposed DBBPF have the measured CFs at the 5.93 and 13.35 GHz with 3 dB fractional bandwidths of 3.45 and 3 GHz (58.2% and 22.5%), while the measured minimum ILs are 0.7 and 0.92 dB, respectively. In Fig. 10 (b), the measured minimum ILs are 0.55 and 1.4 dB in the lower and upper passbands centered at 5.8 and 13.05 GHz with 3 dB relative bandwidths of 58.6% and 20.7%, while two transmission points are generated in the stop band between the lower and upper passbands, respectively. Good agreements between the simulated and measured results are obtained both in the DBBPF and the DBBPF with SIOLRR.

Table 1 illustrates the comparisons of our presented SIW DBBPFs with other reported advanced ones. Compared with the designs in [9]-[11], our proposed ones provide more widely bandwidths, smaller size and widely separated passbands from SIW and BCMRCs technology. Compared to the designs in [12], our proposed DBBPFs provide more widely bandwidths and lower ILs.

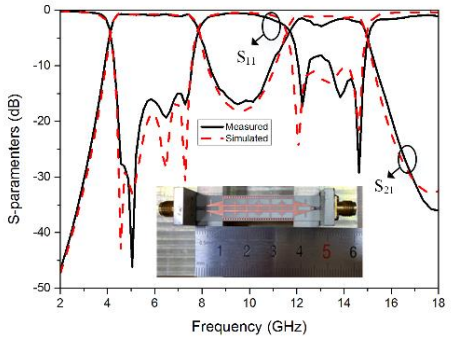

(a)

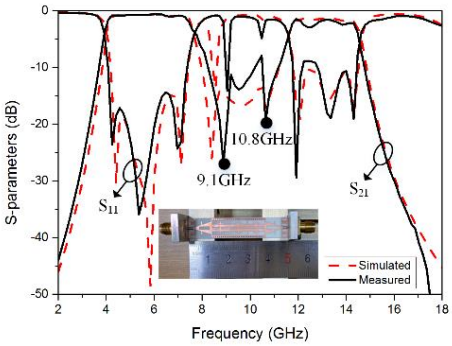

(b)

Fig. 10. Simulated and measured S-parameters of: (a) the DBBP without SIOLRR, and (b) the DBBPF with SIOLRR.

Table 1: Performance comparisons with some previous DBBPFs

	f_1/f_2 (GHz)	$k=f_2/f_1$	3-dB FBW (%) 1st /2nd	IL (dB) 1st /2nd	Size (λ_g^2)
[11]	20/21	1.05	1.5/1.43	1.37/1.1	2.18×1.44
[12]-A	12/14	1.167	5.53/4.04	1.21/1.34	1.15×1.10
[12]-B	12/16	1.333	3.8/3.47	1.79/1.76	2.16×1.25
[13]-A	12/16	1.333	8.75/7.06	1.07/0.95	1.12×1.71
[13]-B	12/15	1.25	7/6.6	1.24/0.85	1.66×1.29
[14]	2.4/5.2	2.25	5.8/6.45	3.6/3.1	0.15×0.16
This work without SIOLRR	**5.9/13.4**	**2.27**	**58.2/22.5**	**0.70/0.92**	**0.26×1.22**
This work with SIOLRR	**5.8/13.1**	**2.26**	**58.6/20.7**	**0.55/1.4**	**0.26×1.35**

IV. CONCLUSION

In this paper, two compact SIW DBBPFs with wide bandwidths and wide separated passbands has been proposed. The structure and design strategy have been analyzed in detail. The SIW provides a highpass performance and the BCMRCs generates a bandstop characteristic. They can be effectively combined to obtain a wideband dual-band filter. Finally, the simulations and measurements of the demonstrative filters are in good agreement, while the measured separated passbands are much wider than those of the previous reported works.

REFERENCES

[1] U. Naeem, S. Bila, M. Thevenot, T. Monediere, and S. Verdeyme, "A dual-band bandpass filter with widely separated passbands," *IEEE Trans. Microw. Theroy Tech.*, vol. 62, no. 3, pp. 450-456, Mar. 2014.

[2] K. D. Xu, H. Luyen, and N. Behdad, "A decoupling and matching network design for single- and dual-band two-element antenna arrays," *IEEE Trans. Microw. Theory Tech.*, vol. 68, no. 9, pp. 3986-3999, Sep. 2020.

[3] J. Shi, L. L. Lin, J. X. Chen, H. Chu, and X. Wu, "Dual-band bandpass filter with wide stopband using one stepped-impedance ring resonator with shorted stubs," *IEEE Microw. Wireless Compon. Lett.*, vol. 24, no. 7, pp. 442-444, July 2014.

[4] Y. J. Guo, X. H. Tang, and K. D. Xu, "Dual high-selectivity band-notched ultra-wideband filter with improved out-of-band rejection," *Applied Computational Electromagnetics Society Journal*, vol. 31, no. 9, pp. 1072-1078, Sep. 2016.

[5] S. Y. Zheng, "A dual-band antenna across microwave and millimeter-wave frequency bands," *2018 International Applied Computational Electromagnetics Society Symposium (ACES)*, Beijing, China, pp. 1-2, Aug. 2018.

[6] Y. Z. Zhu, W. X. Xie, X. Deng, and Y. F. Zhang, "Compact modified quarter mode substrate integrated waveguide resonator and its application to filters design," *Applied Computational Electromagnetics Society Journal*, vol. 32, no. 2, pp. 163-168, Feb. 2017.

[7] D. Li and K. D. Xu, "Compact dual-band bandpass filter using coupled lines and shorted stubs," *Electron. Lett.*, vol. 56, no. 14, pp. 721-724, July 2020.

[8] J. T. Kuo, T. H. Yeh, and C. C. Yeh, "Design of microstrip bandpass filter with a dual-passband response," *IEEE Trans. Microw. Theory Tech.*, vol. 53, no. 4, pp. 1331-1337, Apr. 2005.

[9] S. B. Zhang and L. Zhu, "Synthsis design of dual-band bandpass filters with $\lambda/4$ stepped-impedance resonators," *IEEE Trans. Microw. Theory Tech.*, vol. 61, no. 5, pp. 1812-1819, May 2013.

[10] X. Cao, Z. Tang, and J. Bao, "Design of a dual-band waveguide filter based on micromachining fabrication process," *IET Microw. Antennas Propag.*, vol. 10, no. 4, pp. 459-463, Mar. 2016.

[11] X. P. Chen and K. Wu, "Dual-band and triple-band substrate integrated waveguide filters with chebyshev and quasi-elliptic response," *IEEE Trans. Microw. Theory Tech.*, vol. 55, no. 12, pp. 2569-2578, Dec. 2007.

[12] K. Zhou, C. X. Zhou, and W. Wu, "Resonance characteristics of substrate-integrated rectangular cavity and their applications to dual-band and wide-stopband bandpass filters design," *IEEE Trans. Microw. Theory Tech.*, vol. 65, no. 5, pp. 1511-1524, May 2017.

[13] K. Zhou, C. X. Zhou, and W. Wu, "Substrate-integrated waveguide dual-mode dual-band bandpass filters with widely controllable band-width ratios," *IEEE Trans. Microw. Theory Tech.*, vol. 65, no. 10, pp. 3801-3812, Oct. 2017.

[14] S. S. Xu, K. X. Ma, F. Y. Meng, and K. S. Yeo, "Novel defected ground structure and two-side loading scheme for miniaturized dual-band SIW bandpass filter designs," *IEEE Microw. Wireless Compon. Lett.*, vol. 25, no. 4, pp. 217-219, Apr. 2015.

[15] Y. Dong and T. Itoh, "Miniaturized dual-band substrate integrated waveguide filters using complementary split-ring resonators" *IET Microw. Antennas Propag.*, vol. 6, no. 6, pp. 1-4, June 2011.

[16] P. Li, H. Chu, D. Zhao, and R. S. Chen, "Compact dual-band balanced SIW bandpass filter with improved common-mode suppression," *IEEE Microw. Wireless Compon. Lett.*, vol. 27, no. 4, pp. 347-349, Apr. 2017.

[17] J. C. Rautio, "Publishing at IWS–Part I," *IEEE Microw. Mag.*, vol. 14, no. 4, pp. 162-163, June 2013.

Yun Jiang was born in Hunnan Provence, China. He received the M.S. degrees in Electronic Engineering from the University of Electronic Science and Technology of China (UESTC), Chengdu, China, in 2017, and currently he is working toward the Ph.D. degree in National of Defense University. His research interests include RF/millimeter-wave components and circuits.

Lei Huang was born in 1990. He received the B.S. degree in Vacuum Electronic Technology from University of Electronic Science and Technology of China, Chengdu, China, in 2014, the M.S. degree in Electromagnetic Field and Microwave Technique from National University of Defense Technology, Changsha, China, in 2017. He is currently working toward the Ph.D. degree in Electromagnetic Field and Microwave Technique at the National University of Defense Technology. His current research interests are microwave and millimeter-wave circuits and systems.

Zhaoyu Huang was born in 1992. He received the M.S. degree in Electronics and Communication Engineering from the University of Electronic Science and Technology of China, Chengdu, China in 2018, where he is currently pursuing Ph.D. degree with the College of Electronic Science and Engineering, National University of Defense Technology, Changsha, China. His current research interests include passive RF/microwave circuits, microstrip antennas and wireless communication.

Yuan Ye was born in Guangxi, China. She received the M.S. degree in Sun Yat-sen University, Guangzhou, China, in 2012, and currently she is working toward the Ph.D. degree in National University of Defense Technology. Her current research interests include ultra-wideband antenna Arrays and reconfigurable antenna.

Boyuan Liu was born in 1991. He has received Master's degree from University of Electronic Science and Technology, China and now proceed to Doctor's degree in National University of Defense Technology. His research interests are microwave and millimeter wave circuits and system, Radar guidance, electronic countermeasures and electromagnetic technology. He joined in researches such as Design of Capacitance quickly charging based on the technology of coupling resonance, Design and Implementation of X-band Single Road's Frequency Mixer Channel Based on MEMS Filter, which were finally published on national core periodicals. He is now engaged in one project of Natural Science Foundation of China, named Structure Unit Design of Compound Electromagnetic Material of Graphene Selective Surface, and one innovation project of Research on Multiple-Element Linear Retrodirective Cross-Eye Jamming.

Wentao Yuan was born in 1990. He received his M.S. degree in Computer Science and Technology from the Anhui Normal University in 2016. Currently he is working towards the Ph.D. degree in the College of Electronic Science and Engineering, National University of Defense Technology, Changsha, Hunan, China. His research interests include passive microwave circuits design and wireless communication.

Naichang Yuan was born in Anhui, China, in 1965. He received the M.S. and Ph.D. degrees in Electronic Science and Technology from the University of Electronic Science and Technology of China in 1991 and 1994, respectively. He is currently a Professor with the National University of Defense Technology. His research interests include array signal processing, radar system design, SAR/ISAR imaging and electronic countermeasures.